

Viscous Flow and Jump Dynamics in Molecular Supercooled Liquids: II Rotations

Cristiano De Michele¹ and Dino Leporini^{1,2} [*]

¹ *Dipartimento di Fisica, Università di Pisa, V.Buonarroti, 2 I-56100 Pisa, Italy*

² *Istituto Nazionale di Fisica della Materia, Unità di Pisa*

(Received April 26, 2018)

The rotational dynamics of a supercooled model liquid of rigid A-B dumbbells interacting via a L-J potential is investigated along one single isobar. The orientation correlation functions exhibit a two-step character which evidences molecular trapping. Trapping is also apparent in a suitable angular-velocity correlation functions. The rotational correlation τ_1 is found to scale over more than three orders of magnitude as $(T - T_c)^{-\gamma}$ with $\gamma = 1.47 \pm 0.01$ and T_c the MCT critical temperature. Differently, τ_l with $l = 2 - 4$ and the rotational diffusion coefficient D_r manifest deviations. For $0.7 < T < 2$ good agreement with the diffusion model is found, i.e. $\tau_l \cong 1/l(l+1)D_r$. For lower temperatures the agreement becomes poorer and the results are also only partially accounted for by the jump-rotation model. The angular Van Hove function evidences that in this region a meaningful fraction of the sample reorients by jumps of about 180° . The distribution of the waiting-times in the angular sites cuts exponentially at long times. At lower temperatures it decays at short times as $t^{\xi-1}$ with $\xi = 0.34 \pm 0.04$ at $T = 0.5$ in analogy with the translational case. The breakdown of the Debye-Stokes-Einstein is observed at lower temperatures where the rotational correlation times diverge more weakly than the viscosity.

PACS numbers: 64.70.Pf, 02.70.Ns, 66.20.+d , 66.10.-x

I. INTRODUCTION

The relaxation and the transport properties of molecular liquids depend on both their translational and rotational motion. Since their mutual interplay cannot be neglected both dynamical aspects must be jointly considered. If the liquids are supercooled or supercompressed the overwhelming difficulties to molecular rearrangement are expected to enhance the role of the rotational degrees of freedom and, more particularly, the rotational-translational coupling as noticed by experiments [1–5], theory [6–8] and numerical [9–12] studies and discussed in a recent topical meeting [13].

Molecular-dynamics numerical (MD) studies provided considerable insight in supercooled liquids during the last years [14]. However, the question of rotational dynamics seems to have been partially overlooked since most studies dealt with atomic systems where rotational dynamics is missing. Notable exceptions addressed the issue in model systems of disordered dipolar lattice [9], biatomic molecules [10,11] and well studied glassformers, e.g. CKN [15], OTP [16,17] and methanol [18]. The case of supercooled water was investigated in detail [19]. Studies of plastic crystals and orientational glasses (i.e. no allowed translation) are also known [20,21].

We have recently presented numerical results on the translational motion of a supercooled molecular model liquid [22] (hereafter referred to as I). The present paper wishes to complement I by extending the analysis to rotational degrees of freedom. As in I one issue is the detection and characterization of jump dynamics. It is found that rotational jumps are fairly more frequent than

translational ones in the present system. This makes it easier their study. The occurrence of jumps poses the question of the coupling of the molecular reorientation with the shear viscous flow. This is the second issue addressed in the paper. Jump dynamics may take place in the absence of any shear flow. Nonetheless, shear motion may favour jumps over energy barriers [23]. The question is of relevance in that the experimental situation is rather controversial. For macroscopic bodies hydrodynamics predicts that the reorientation is strongly coupled to the viscosity η according to the Debye-Stokes-Einstein law (DSE), $\tau, D_r^{-1} \propto \eta$, where τ and D_r are the rotational correlation time and diffusion coefficient, respectively [24–26]. DSE is quite robust. In fact, the coupling of the reorientation to the viscosity is usually found even at a molecular level if the viscosity is smaller of about 1–10 *Poise*. At higher values DSE overestimates the correlation times of tracers in supercooled liquids according to time-resolved fluorescence [27,28] and Electron Spin Resonance (ESR) studies [5,29,30]. On the other hand, photobleaching [2] and NMR [3] studies found only small deviations from DSE even close to T_g . Interestingly, according to ESR studies in the region where tracer reorientation decouples by the viscosity, an ESR study evidenced that it occurs by jump motion [31,32].

The paper is organized as follows. In section II details are given on the model and the simulations. In Sec. III and IV the results are discussed and the conclusions are summarized, respectively.

II. MODEL AND DETAILS OF SIMULATION

The system under study is a model molecular liquid of rigid dumbbells [10–12]. The atoms A and B of each molecule have mass m and are spaced by d . Atoms on different molecules interact via the Lennard-Jones potential:

$$V_{\alpha\beta}(r) = 4\epsilon_{\alpha\beta} \left[(\sigma_{\alpha\beta}/r)^{12} - (\sigma_{\alpha\beta}/r)^6 \right], \quad \alpha, \beta \in \{A, B\} \quad (1)$$

The potential was cutoff and shifted at $r_{cutoff} = 2.49\sigma_{AA}$. Henceforth, reduced units will be used. Lengths are in units of σ_{AA} , energies in units of ϵ_{AA} and masses in units of m . The time unit is $\left(\frac{m\sigma_{AA}^2}{\epsilon_{AA}}\right)^{1/2}$, corresponding to about $2ps$ for the Argon atom. The pressure P , temperature T and shear viscosity η are in units of $\epsilon_{AA}/\sigma_{AA}^3$, ϵ_{AA}/k_B and $\sqrt{m\epsilon_{AA}}/\sigma_{AA}^2$, respectively.

The model parameters in reduced units are: $\sigma_{AA} = \sigma_{AB} = 1.0$, $\sigma_{BB} = 0.95$, $\epsilon_{AA} = \epsilon_{AB} = 1.0$, $\epsilon_{BB} = 0.95$, $d = 0.5$, $m_A = m_B = m = 1.0$. The σ_{AA} and σ_{BB} values were chosen to avoid crystallization. The sample has $N = N_{at}/2 = 1000$ molecules which are accommodated in a cubic box with periodic boundary conditions. Further details on the simulations may be found in I.

We examined the isobar at $P = 1.5$ by equilibrating the sample under isothermal-isobaric conditions and then collecting the data by a production run in microcanonical conditions. The temperatures we investigated are $T = 6, 5, 3, 2, 1.4, 1.1, 0.85, 0.70, 0.632, 0.588, 0.549, 0.52, 0.5$.

III. RESULTS AND DISCUSSION

This section will discuss the results of the study. We characterize the correlation losses of the system by investigating several rotational correlation functions. Then, the related correlation times and transport coefficients will be presented. The presence of rotational jumps will be evidenced and their waiting time distribution will be discussed. Finally, the decoupling of the transport and the relaxation from the viscous flow will be presented.

A. Correlation Functions

The rotational correlation loss is conveniently presented by suitable correlation functions. We study the dynamics of both the orientation and the angular velocity of the dumb-bell.

1. Orientation

The rotational correlation functions are defined:

$$C_l(t) = \frac{1}{N} \sum_{i=1}^N \langle P_l(\mathbf{u}_i(t) \cdot \mathbf{u}_i(0)) \rangle \quad (2)$$

$\mathbf{u}_i(t)$ is the unit vector parallel to the axis of the molecule i at time t and $P_l(x)$ the Legendre polynomial of order l . It is worth noting that C_1 and C_2 are accessible to several experimental techniques, e.g. dielectric spectroscopy, NMR, ESR, light and neutron scattering.

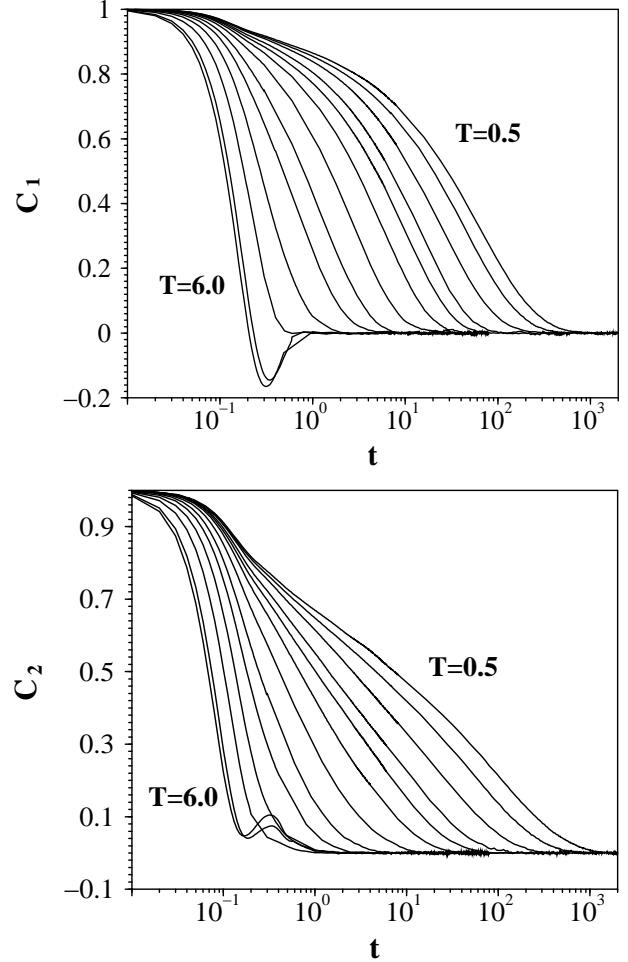


FIG. 1. Correlation functions C_1 and C_2 plotted for all the temperatures investigated.

Fig. 1 shows C_1 and C_2 . At high temperature and short times damped oscillations are present. They are typical features of free rotators in gas-like systems [20,33]. At lower temperatures and intermediate times C_1 and C_2 exhibit a wide plateau which evidences the increased angular trapping. At longer times the decay is fairly well described by the stretched exponential $\sim \exp[-(t/\tau)^\beta]$ with $\tau = 62.9$, $\beta = 0.70$ for $l = 1$ and $\tau = 96.1$, $\beta = 0.60$ for $l = 2$ at $T = 0.5$. Even if C_1 and C_2 are quite similar two differences must be noted. First the plateau is lower at $l = 2$ than at $l = 1$. Second, at lower temperatures C_2 vanishes at longer times than C_1 . The first feature is understood by noting that the oscillatory character of

$P_l(\mathbf{u}_i(t) \cdot \mathbf{u}_i(0))$ with respect to the angle between $\mathbf{u}_i(t)$ and $\mathbf{u}_i(0)$ increases with l . Then, by increasing l even random angular changes with small amplitude occurring at short times affect the decay of C_l . The second feature is due to the fact that, as it will be shown later, molecules undergo frequent 180° flips at lower temperatures. Due to the nearly head-tail symmetry, the flips reverse the sign of $P_l(\mathbf{u}_i(t) \cdot \mathbf{u}_i(0))$ if l is odd whereas no change takes place if l is even. Then, they mainly affect the decay of C_l with odd l values.

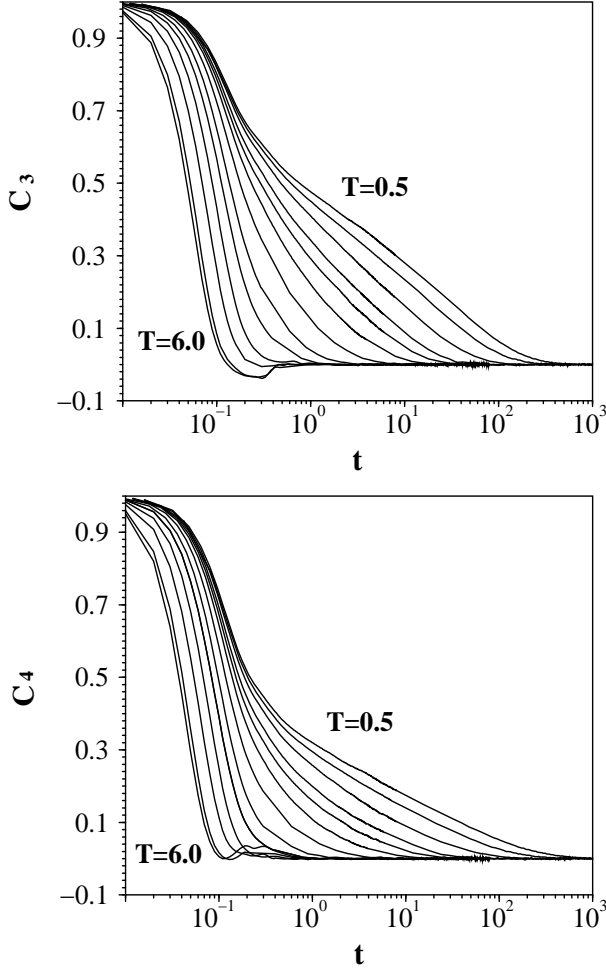


FIG. 2. Correlation functions C_3 and C_4 for all the temperatures investigated.

Fig. 2 plots the functions C_3 and C_4 . The discussion is similar to the case $l = 1, 2$. We note that, as expected, the plateau decreases by increasing l . On the basis of the above discussion C_3 should vanish before C_4 . However, on increasing l , the effect of the head-tail symmetry is partially masked by the increased oscillatory character of the Legendre polynomials, which yields a larger sensitivity to small-angle reorientations. Similarly to $C_{1,2}$ at longer times the decay is fairly well described by the stretched exponential $\sim \exp[-(t/\tau)^\beta]$ with $\tau = 32.4$, $\beta = 0.60$ for $l = 3$ and $\tau = 27.9$, $\beta = 0.47$ for $l = 4$

at $T = 0.5$. We notice that the stretching parameter decreases with increasing l .

Fig. 3 compares the four correlation functions C_l with $l = 1 - 4$ at $T = 0.5$ are shown. Both the larger correlation loss at short times at larger l values and the odd-even effect on the long-time decay of the correlations are evidenced.

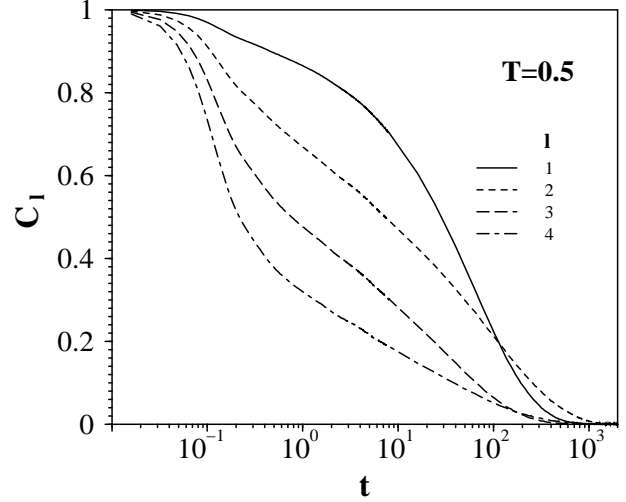


FIG. 3. Correlation functions C_1, C_2, C_3 and C_4 at $T = 0.5$. C_l decay more at short times by increasing l . The curves with $l = 1, 3$ decay faster at long times than the curves with $l = 2, 4$, respectively, due to the partial head-tail symmetry of the molecules.

2. Angular velocity

For a linear molecule the angular velocity is:

$$\boldsymbol{\omega} = \mathbf{u} \times \dot{\mathbf{u}} \quad (3)$$

A set of correlation functions is defined as:

$$\Psi_l(t) = \frac{1}{N} \sum_{i=1}^N \langle P_l(\cos \alpha_i(t)) \rangle, \quad l \geq 1, \quad (4)$$

$\alpha_i(t)$ is the angle between $\boldsymbol{\omega}_i(t)$ and $\boldsymbol{\omega}_i(0)$. In particular, for $l = 1$ one has:

$$\Psi_1 = \frac{\langle \boldsymbol{\omega}(0) \cdot \boldsymbol{\omega}(t) \rangle}{\langle |\boldsymbol{\omega}|^2 \rangle} \quad (5)$$

which is the usual correlation function of the angular velocity. In fig. 4 Ψ_1 and Ψ_2 are drawn for all temperatures investigated. Ψ_1 decays fast and increasing T slows down the decay (note the difference with the orientation case). In particular, in the free-rotator limit Ψ_1 is a constant. At lower temperatures Ψ_1 shows a negative part at short times which evidences a change of sign of $\boldsymbol{\omega}$. This must be ascribed to the collisions on the rigid cage trapping the molecule (see figs. 1 and 2). An analogous effect was

also noted for the linear velocity correlation function in I. More insight on the rotational trapping may be gained by inspecting Ψ_2 in fig.4. No significant differences between Ψ_2 and Ψ_1 are seen at high temperature. At lower temperatures, after a similar ballistic initial decay of Ψ_1 and Ψ_2 , the latter slows down when $\Psi_2 \approx 0.25$. The long-living tail which shows up is interpreted by noting that at lower temperatures, after the ballistic regime the angular velocity is approximately trapped in a circle (see eq.3). An elementary calculation shows that $\Psi_1(t) = 0$ whereas $\Psi_2(t) = 0.25$ as long as the trapping is effective [20]. When the molecular rearrangement allows the orientation relaxation, the angular velocity tends to be distributed over a sphere and Ψ_2 vanishes approximately as C_2 .

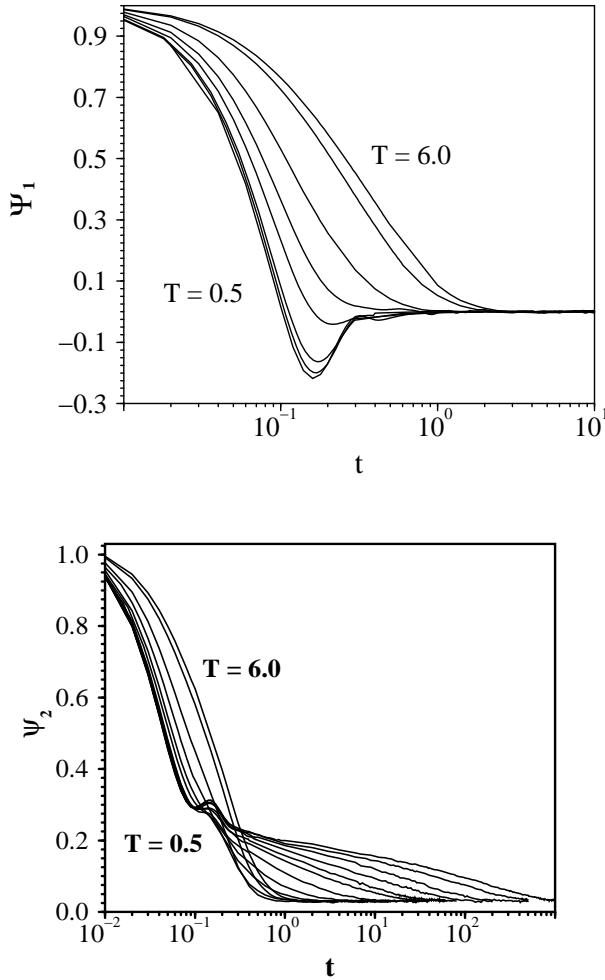


FIG. 4. Correlation functions of the angular velocity Ψ_1 and Ψ_2 plotted for all the temperatures studied.

B. Diffusion coefficient and relaxation times

The rotational diffusion coefficient of a linear molecule may be defined by a suitable Green-Kubo formula in close analogy to the translational counterpart as [33]:

$$D_r = \frac{1}{2} \int_0^\infty \langle \omega(0) \cdot \omega(t) \rangle dt \quad (6)$$

From a computational point of view the evaluation of the above integral is delicate and it is more convenient to evaluate D_r via the Einstein relation

$$D_r = \lim_{t \rightarrow \infty} \frac{R_r}{4t} \quad (7)$$

R_r is the mean squared angular displacement :

$$R_r(t) = \frac{1}{N} \sum_{i=1}^N \langle |\phi_i(t + t_0) - \phi_i(t_0)|^2 \rangle \quad (8)$$

where $\phi_i(t)$ is :

$$\phi_i(t) - \phi_i(0) = \Delta\phi_i(t) = \int_0^t \omega_i(t') dt' \quad (9)$$

In Fig. 5 $R_r(t)$ is shown. The plots are qualitatively similar to the mean squared translational displacement (see I). At short time the motion is ballistic. At intermediate times and lower temperatures a plateau shows up. It signals the increasing trapping of the molecular orientation due to the severe constraints on the structure relaxation. At longer times the reorientation is diffusive according to eq.7. By comparing $R_r(t)$ with the translational mean square displacement (see fig.3 of I) it is seen that the angular trapping is weaker than the one affecting the center-of-mass motion since the subdiffusive intermediate regime is less pronounced and extends less on the time scale.

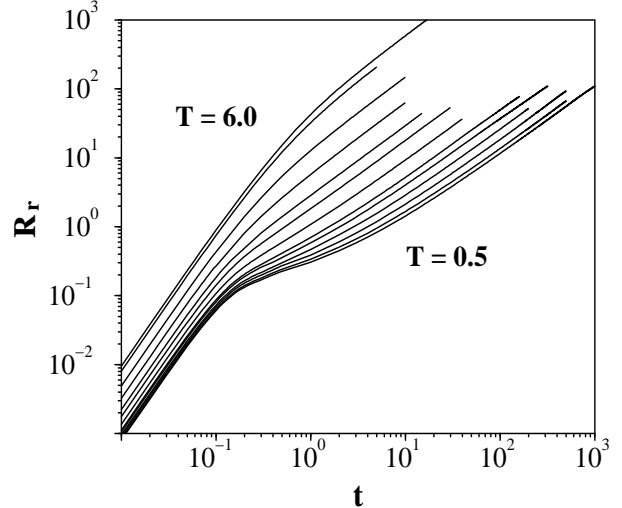


FIG. 5. Mean squared angular displacement for all the temperatures investigated.

The rotational correlation times are defined as [33]:

$$\tau_l = \int_0^\infty C_l(t) dt \quad (10)$$

Fig. 6 presents the T-dependence of τ_l , $l = 1 - 4$ and D_r . It is seen that a wide region exists where the above quantities exhibit approximately the same Arrhenius behavior (about $0.7 < T < 2$). At lower temperatures the apparent activation energy of the rotational correlation times increase. In particular, as noted in Sec.III A 1, τ_1 becomes shorter than τ_2 and a similar crossover is anticipated between τ_3 and τ_4 at temperatures just below 0.5. Differently, the rotational diffusion coefficient D_r exhibits the same activated behavior over a region which was shown to extend also below the critical temperature T_c predicted by the mode-coupling theory (MCT) [10]. The decoupling of D_r with respect to τ_l may be anticipated by noting that the former is related to the area below $\Psi_1(t)$ (eq.7) and the latter to the area below $C_l(t)$ (eq.10). At lower temperatures $\Psi_1(t)$ vanishes faster so probing the fast dynamics of the supercooled liquid whereas the decay of $C_l(t)$ slows down more and more (see Sec. III A). Alternatively, it has to be noted that even in highly-constrained liquids small angular motions which are unable to relax the orientation lead to a finite value of D_r in view of eq. 7 [10]. Such librational motions were detected in an MD study of OTP [16].

Fig. 6 shows also the MCT analysis of the T-dependence of the correlation time and the rotational diffusion [6,7]. According to MCT, both τ_l and D_r should scale as

$$\tau_l, D_r^{-1} \propto (T - T_c)^{-\gamma} \quad (11)$$

The underlying expectation on the scaling 11 is that it should work with the same T_c value for any transport coefficient and relaxation time. Differently, the physical meaning of T_c could be weakened. In I it was shown that eq.11 fits the divergence of the translational diffusion coefficient D over four orders of magnitude with $T_c = 0.458 \pm 0.002$ and $\gamma_D = 1.93 \pm 0.02$ (the data are partially shown in fig. 6) and that at lower temperatures the primary relaxation time $\tau_\alpha \propto D^{-1}$. Fig. 6 shows that the scaling 11 is also effective for τ_1 with $\gamma = 1.47 \pm 0.01$ (see also fig.7). However, meaningful deviations are apparent for $l \geq 2$ and D_r . The deviations increase as l increases. Since the rotational correlation functions C_l are more and more sensitive to small-amplitude reorientations and then to small molecular displacements, the poorer scaling may be a consequence of the difficulties of the mode-coupling theories at short distances [34,35].

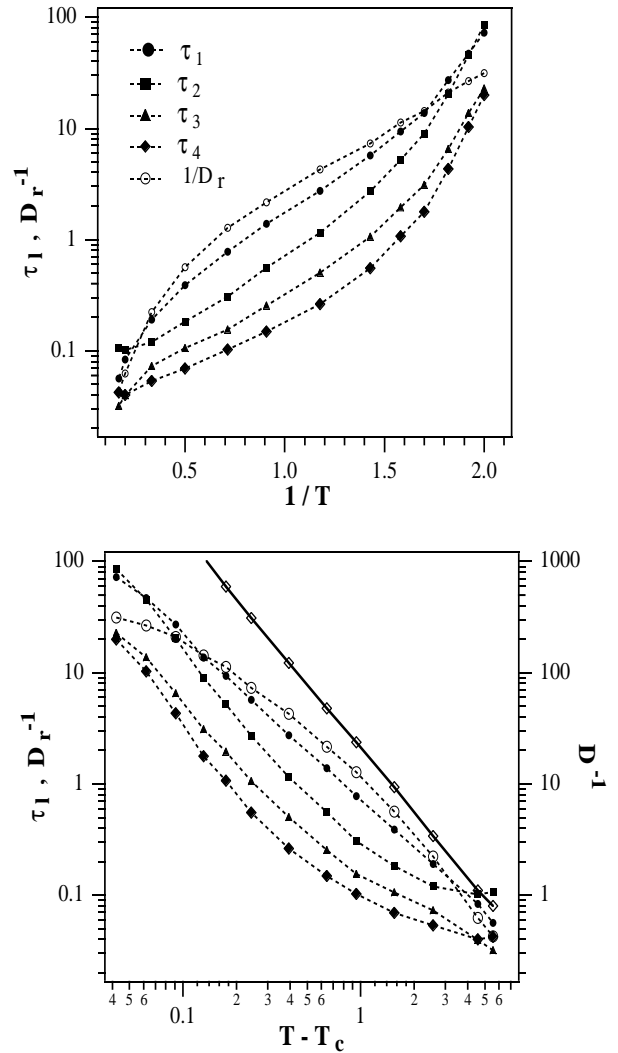


FIG. 6. Arrhenius plot (top) and MCT scaling analysis (bottom) of the rotational correlation times τ_l , $l = 1 - 4$ and the rotational diffusion coefficient D_r . $T_c = 0.458$. The dashed lines are guides for the eyes. The translational diffusion constant D is also drawn for comparison (open diamonds). The continuous line is the best fit by using eq.11 with $\gamma_D = 1.93 \pm 0.02$.

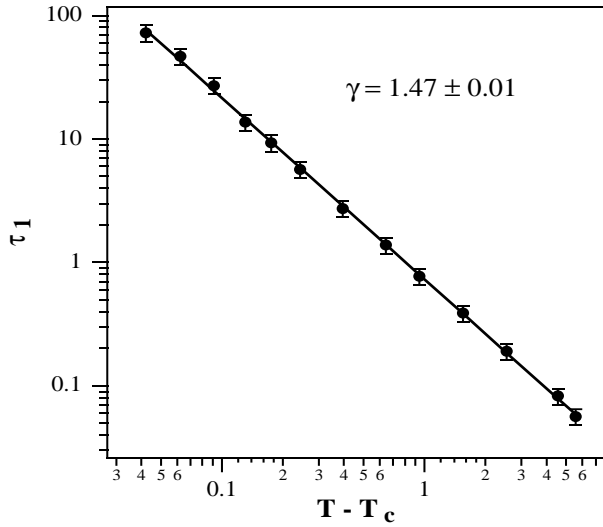


FIG. 7. MCT scaling analysis of τ_1 . $T_c = 0.458$.

To characterize the reorientation process, we studied the quantity $l(l+1)D_r\tau_l$ and the ratio $l(l+1)\tau_l/2\tau_1$. If the molecule rotates by small angular jumps, or equivalently the waiting time in a single angular site is fairly shorter than the correlation time τ_l , the motion is said to be diffusive and both quantities are equal to 1 for any l value [25,33]. The results are shown in fig.8. Three regions may be broadly defined. For $T > 2$ the properties are gas-like and the rotational correlation times become fairly long. For $0.7 < T < 2$ $l(l+1)D_r\tau_l$ and $l(l+1)\tau_l/2\tau_1$ do not change appreciably and are in the range 1–2. For $T < 0.7$ the above quantities diverge abruptly. The rapid increase in the deeply supercooled regime demonstrates the failure of the diffusion model which in fact is expected to work only in liquids with moderate viscosity or if the reorientating molecule is quite large. If the assumption of small angular jumps is released and proper account of finite jumps with a single average waiting time in each angular site is made, the so-called jump-rotation model is derived [32]. The main conclusion is that τ_l is roughly independent of l . In fact, for $l = 2$ it is found that the quantity $l(l+1)\tau_l/2\tau_1 \approx 3.5$ at $T = 0.5$ (see fig.8) and the jump-rotation model predicts a value of about 3. However, at higher l values the comparison becomes much less favourable. For $l = 3$ $l(l+1)\tau_l/2\tau_1 \approx 1.9$ at $T = 0.5$ whereas the prediction is about 6. For $l = 4$ $l(l+1)\tau_l/2\tau_1 \approx 2.75$ to be compared to the prediction is about 10. The failure of the usual simple rotational models is not unexpected. Their basic assumptions are rather questionable in supercooled liquids, e.g. the inherent homogeneity of the liquid and the presence of a single time scale both leading to the simple exponential decay of the rotational correlation functions.

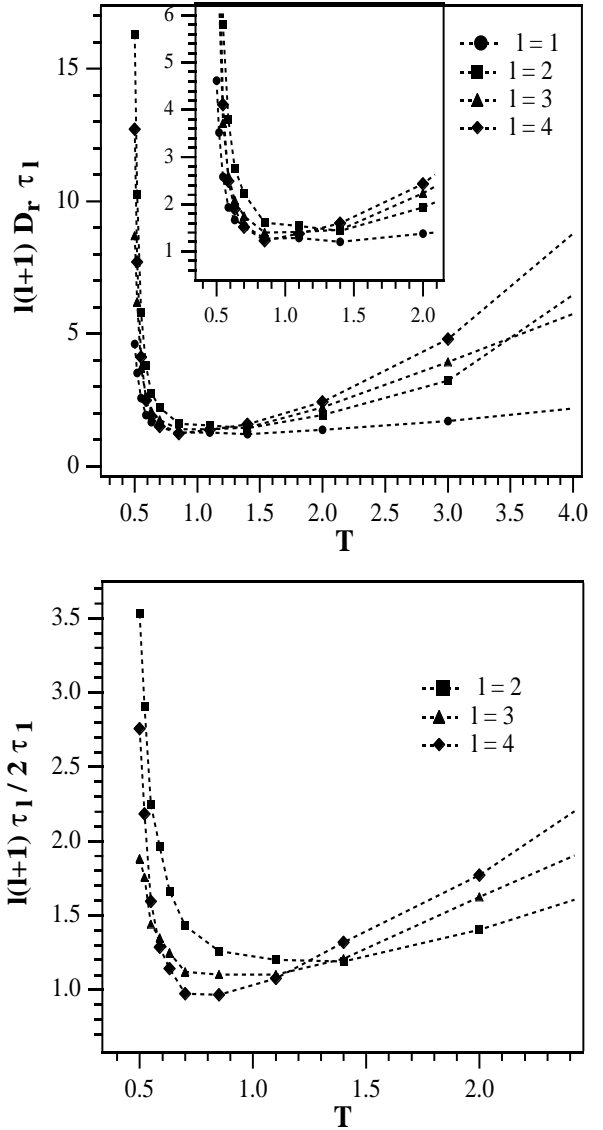


FIG. 8. Temperature dependence of the quantity $l(l+1)D_r\tau_l$ for $l = 1, 2, 3, 4$ (top) and the ratio $l(l+1)\tau_l/2\tau_1$ for $l = 2, 3, 4$ (bottom). If the reorientation is diffusive both quantities must be equal to 1. If the reorientation is jump-like $\tau_l \approx \tau_1$.

C. Jump rotation

The inadequate description provided by the diffusion and the jump model calls for a further characterization of the rotational motion. To this aim we consider the self-part of the angular Van Hove function:

$$G_s^\theta(\theta, t) = \frac{2}{N \sin \theta} \sum_{i=1}^N \delta(\theta - \theta_i(t)) \quad (12)$$

$\theta_i(t)$ is the angle between the molecular axis of the i -th molecule at the initial time and time t . $1/2G_s^\theta(\theta, t)\sin\theta d\theta$ is the probability to have the axis of a

molecule at angle between θ and $\theta + d\theta$ at time t with respect to the initial orientation. At long times $G_s^\theta(\theta, t) \cong 1$ since all the orientations are equiprobable.

In Fig. 9 the function G_s^θ is plotted for different temperatures and several times. At higher temperatures, as the time goes by, the molecule explores more and more angular sites in a continuous way. Instead, at lower temperatures G_s^θ exhibits a peak at $\theta \approx 180^\circ$ and intermediate times signaling that the reorientation has a meaningful probability to occur by jumps.

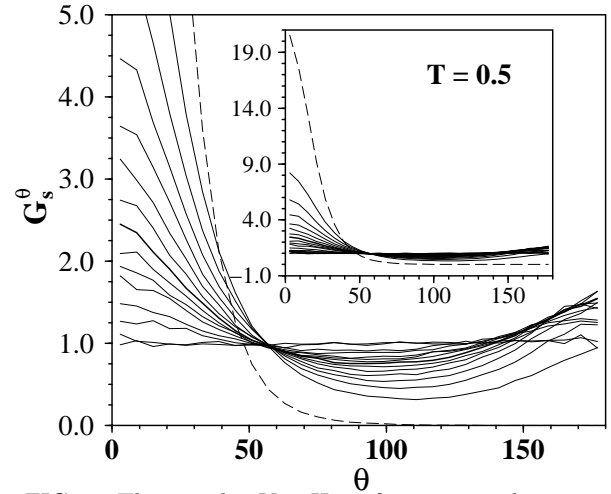
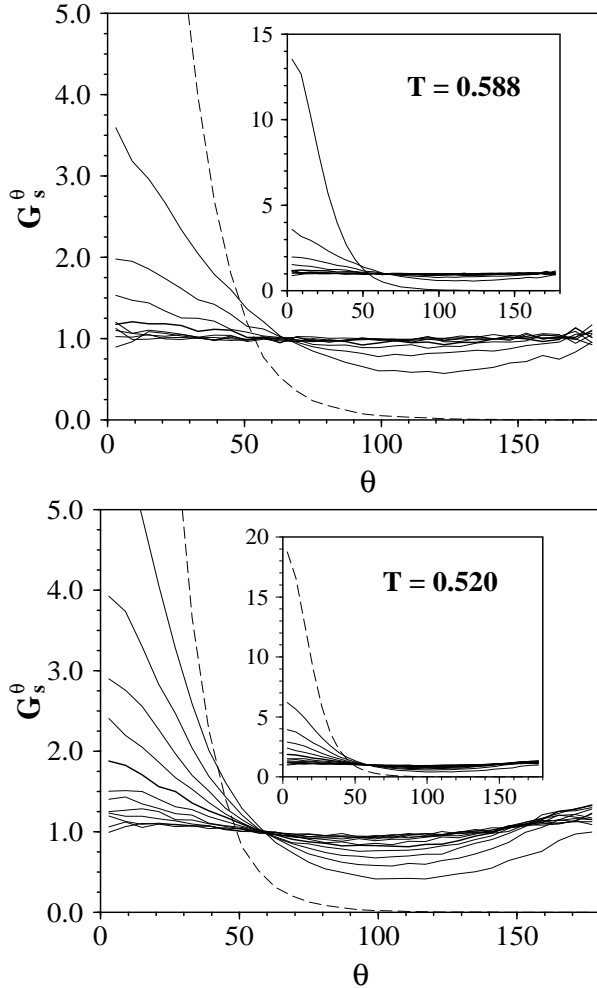


FIG. 9. The angular Van Hove functions at low temperatures. Top: $T = 0.588$, bold line $t = 80$. Middle: $T = 0.520$, bold line $t = 200$. Bottom: $T = 0.5$, bold line $t = 280$. Dashed line $t = 1$. The other continuous lines are plotted at intermediate times with equal spacing.

The indications provided by the VanHove function concerning the presence of rotational jumps are confirmed by directly inspecting the single particles trajectories (fig. 10). Similar findings were reported also in other studies on dumbbells and CKN glassformers [10,15]. With respect to the translational counterparts, it must be pointed out that they are quite faster (see I) and more frequent (about one order of magnitude). The higher number of rotational jumps is also anticipated by noting that, differently from the translational Van-Hove function, the rotational one does exhibit explicit signatures of jump motion (see I).

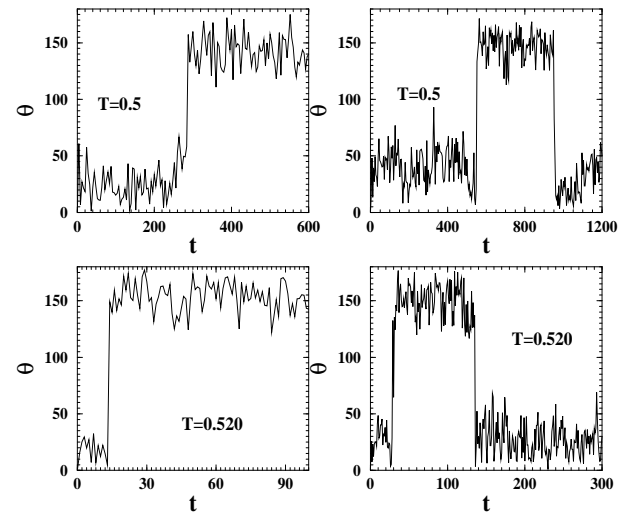


FIG. 10. Selected single-particle orientations evidencing the flips occurring at low temperatures.

To characterize the jumps we studied the distribution $\psi_{rot}(t)$ of the waiting-time, namely the residence time in

one angular site of the unit vector \mathbf{u}_i being parallel to the axis of the i -th molecule. A jump of the i -th molecule is detected at t_0 if the angle between $\mathbf{u}_i(t_0)$ and $\mathbf{u}_i(t_0 + \Delta t^*)$ is larger than 100° with $\Delta t^* = 24$. To prevent multiple countings of the same jump, the molecule which jumped at time t is forgotten for a lapse of time Δt^* . To minimize possible contributions due to fast rattling motion, each angular displacement is averaged with the previous and the next ones being spaced typically by 6–8 time units, depending on the temperature. The jump search procedure was validated by inspecting several single-molecule trajectories. The above definition of rotational jump fits well their general features, i.e. they are rather fast and exhibit no meaningful distribution of both the amplitude and the time needed to complete a jump (see fig.10). It is worth noting that in I it was found that the time needed to complete the translational jumps exhibits a distribution. The absence of a similar distribution for the rotational jumps points to a larger freedom of the latter.

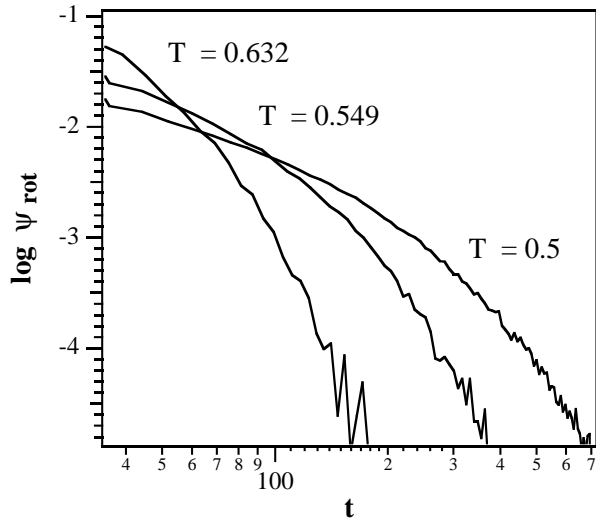


FIG. 11. The rotational waiting-time distribution $\psi_{rot}(t)$ at low temperatures.

Fig.11 shows $\psi_{rot}(t)$ at different temperatures. At $T = 0.632$ is virtually exponential. At lower temperatures deviations become apparent which are analyzed for $T = 0.5$ in fig. 12. In I it was noted that the translational waiting-time distribution may be fitted nicely by the truncated power law:

$$\psi(t) = [\Gamma(\xi)\tau^\xi]^{-1} t^{\xi-1} e^{-t/\tau} \quad 0 < \xi \leq 1 \quad (13)$$

The best fit provided by eq.13 is compared to the fits by using the stretched ($\exp[-(t/\tau)^\beta]$) and the usual exponential functions in fig. 12. The better agreement of eq.13 at short times may be appreciated by looking at the residuals.

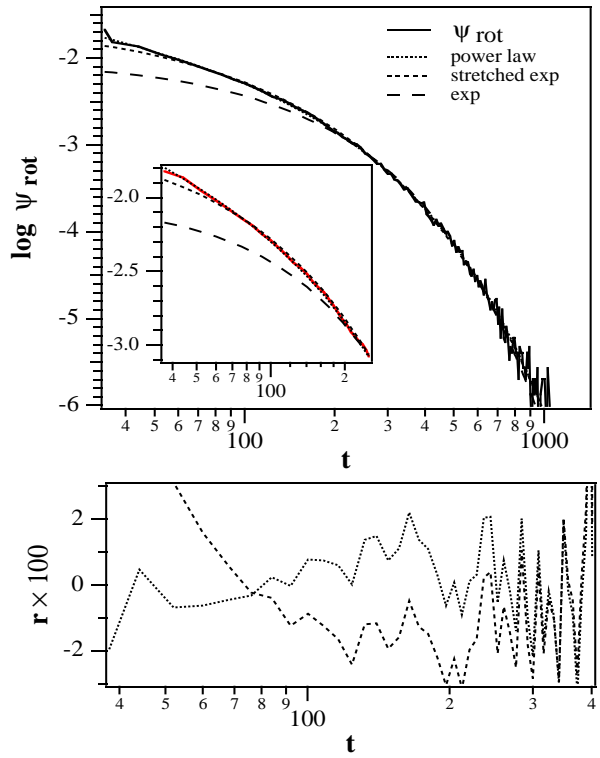


FIG. 12. Analysis of the rotational waiting-time distribution ψ_{rot} at $T = 0.5$. Top: comparison of the best fits with the exponential ($\tau = 102 \pm 3$), the stretched exponential (stretching $\beta = 0.78 \pm 0.02$ and $\tau = 63 \pm 4$) and the truncated power law eq.13 ($\xi = 0.34 \pm 0.04$ and $\tau = 125 \pm 3$). The insert is a magnification of the short-time region. Notice that the fit with the power law is virtually superimposed to ψ_{rot} . Bottom: residuals of the fits in terms of the truncated power law and the stretched exponential.

The fractal behavior of both the translational and the rotational waiting-time distributions is an indication that the molecular motion at short times exhibits intermittent behavior. The issue in the framework of glasses has been addressed by several authors [36–40]. The exponent ξ of eq.13 has a simple interpretation. If a dot on the time axis marks a jump, the fractal dimension of the set of dots is ξ . For $\xi < 1$, it follows $\psi(t) \propto t^{\xi-1}$ at short times [36,41] in agreement with our results. If $\xi = 1$, the distribution of dots is uniform and $\psi(t)$ recovers the exponential form. This is expected beyond a time scale τ and the exponential decay of $\psi_{rot}(t)$ at long times signals the crossover to the usual Poisson regime. It must be noted that the translational waiting time distribution at the lowest temperature ($T = 0.5$) shows a weak tendency to vanish faster than eq.13. A similar feature is not observed in $\psi_{rot}(t)$.

D. Breakdown of the Debye-Stokes-Einstein Law

For large Brownian particles the reorientation in a liquid occurs via a series of small angular steps, i.e. it

is diffusive. Hydrodynamics predicts that the diffusion manifests a strong coupling to the viscosity η which is accounted for by the Debye-Stokes-Einstein law (DSE). For biaxial ellipsoids it takes the form [25]

$$D_i = \frac{kT}{\mu_i \eta}, \quad i = x, y, z \quad (14)$$

$D_{x,y,z}$ are the principal values of the diffusion tensor, k is the Boltzmann constant. The coefficients μ_i depend on the geometry and the boundary conditions (BC). For a sphere with stick BC $\mu_{x,y,z} = 6v$, v being the volume of the sphere. For an uniaxial ellipsoid one considers $D_{\parallel} = D_z$ and $D_{\perp} = D_x = D_y$. The case of stick BC can be worked analytically [24,25]. For slip BC numerical results for D_{\perp} are known [26] (note that in this case the fluid does not exert torques parallel to the symmetry axis). Eq.14 is sometimes rewritten in an alternative form in terms of proper rotational correlation times, e.g. for uniaxial molecules the equality $\tau_l = 1/l(l+1)D_{\perp}$ holds. The new form is more suitable for comparison with the experiments since they do not usually provide direct access to the rotational diffusion coefficients.

Irrespective of the heavy hydrodynamic assumptions, DSE works nicely even at a molecular level if the viscosity is not high ($\eta < 1 \text{ Poise}$). Deviations are observed at higher viscosities for tracers in supercooled liquids by time-resolved fluorescence [27,28] and Electron Spin Resonance (ESR) studies [5,29,30]. On the other hand, photobleaching [2] and NMR [3], studies found only small deviations from DSE even close to T_g . In all the cases known, DSE is found to overestimate the rotational correlation times since on cooling their increase is less than the one being exhibited by the viscosity. In this decoupling region ESR evidenced that the tracer under investigation rotates by jump motion [31].

Shear motion facilitates molecular jumps over energy barriers [23]. On the other hand, guest molecules may jump in frozen hosts in the absence of viscous flow. Since a meaningful fraction of the molecule in the system reorients by finite angular steps with intermittent behavior, not quite expected in a liquid, it is of interest to investigate to what extent the reorientation is coupled to the viscous shear flow.

The results are shown in fig. 13 by plotting the quantity η/XkT with $X = D_r^{-1}$, $l(l+1)\tau_l$ with $l = 1 - 4$. According to DSE it should be constant. The viscosity data were taken from I. At high temperatures the quantity approaches the value expected for stick BC. For $T > 5$ a tendency of η/XkT for $X = D_r, \tau_1$ to increase is noted. However, at such temperatures the system manifests gas-like features (see figs.1,2,4). On cooling η/XkT increases. For intermediate temperatures the liquid properties are well developed, the system is diffusive ($l(l+1)\tau_l D_r \approx 1$, see fig.8) and η/XkT has a value close to the DSE expectation with slip BC. Notably, $D_r \eta/kT$ remains close to this value in the wide interval $2 < T < 6$. At lower temperatures η/XkT diverges. The stronger deviations are exhibited by D_r and

τ_1 , the weaker ones by τ_2 . τ_3 and τ_4 track the behavior of τ_1 and τ_4 , respectively, being the pair $\tau_{1,3}$ being affected by the jump motion much more than the pair $\tau_{2,4}$ (see sec.III A 1. η increases of a factor of about 400 between $T = 1.4$ and 0.5. The corresponding changes of $D_r \eta/kT$, $\eta/\tau_1 kT$ and $\eta/\tau_2 kT$ are 41, 11 and 3.6, respectively. The discussion support the conclusion that the correlators being affected by rotational jumps, e.g. $C_{1,3}(t)$, yield correlation times fairly more decoupled by the viscosity.

If one compares the changes of $\eta/\tau_2 kT$ to the ones drawn by ESR and fluorescence experiments in the region $T/T_c \approx 1.1 - 1.5$, a broad agreement is found [27,5]. These experiments found even larger values of $\eta/\tau_2 kT$ on approaching T_g . Instead, photobleaching studies detected changes of less than order of magnitude by changing η over about 12 orders of magnitude which are extremely smaller than the present ones [2].

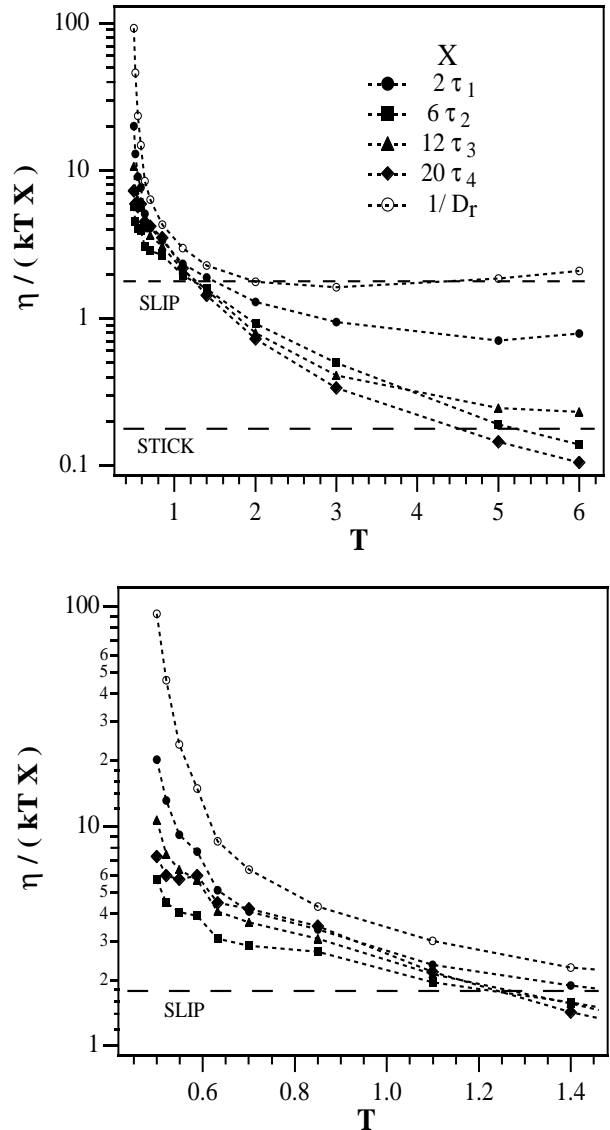


FIG. 13. Plots of the quantity η/XkT with $X = D_r^{-1}, l(l+1)\tau_l$ over the overall temperature range (top) and in the supercooled regime (bottom). According to DSE, the quantity is a constant whose value depends on the hydrodynamic boundary conditions. The superimposed dashed lines are the DSE expectations for stick and slip boundary conditions. Notice that at $T = 1.4$ η/XkT depends little on X , signaling diffusive behavior.

Inspection of fig.13 suggests a way to reconcile, at least partially, the ESR [5], the photobleaching [2] and NMR [3] studies on the glass former o-terphenyl (OTP). Both photobleaching and NMR measure τ_2 in a direct way. Instead, in the glass transition region the ESR lineshape depends in principle on several τ_l and a model is needed to relate them to each other and lead to τ_2 [31]. The model is adjusted by fitting the theoretical prediction with the highly structured ESR lineshape. Fig.13 shows that the decoupling, as expressed by $\eta/\tau_l kT$ increases with l . Since the weight of the τ_l to set the ESR lineshape is roughly comparable, one may anticipate that τ_2^{ESR} may be underestimated at some degree around the glass transition. On the other hand, it must be pointed out that the rotational decoupling is observed up to $1.4T_g$ in OTP where ESR yields τ_2 in a model-independent way [5]. Furthermore, the decoupling is evidenced also by fluorescence experiments which provide τ_2 in a model-independent way [27].

IV. CONCLUSIONS

The present paper investigated the rotational dynamics of a supercooled molecular system. The study addressed several general features and focussed on the characterization of the jump dynamics and the degree of coupling with the viscosity.

The ensemble consists of rigid A-B dumbbells interacting via a L-J potential. All the properties were studied along the isobar $P = 1.5$. The time orientation correlation functions $C_l(t)$ exhibit at high temperatures gas-like features. In the supercooled regime, after a first initial decay, a plateau is observed which signals the trapping of the molecule due to the increased difficulty of the surroundings to rearrange themselves. The plateau level decreases by increasing the l rank of the correlation function due to the larger sensitivity to small-angle librations. The long-time decay of $C_l(t)$ is fairly well described by a stretched exponential. The stretching increases from $l = 1$ ($\beta = 0.7$) to $l = 4$ ($\beta = 0.47$) at $T = 0.5$. The influence on the decay time of C_l (and then on τ_l) of the partial head-tail symmetry of the dumbbells was noted.

A set of angular-velocity correlation functions Ψ_l was defined. Ψ_1 decays faster and faster on decreasing T . Differently, Ψ_2 develops a long-lasting tail which vanishes on the time scale of C_2 .

The temperature dependence of the rotational correlation times τ_l with $l = 2-4$ and the rotational diffusion co-

efficient D_r manifest deviations by the power-law scaling in $T - T_c$, being T_c the MCT critical temperature. There were ascribed to the difficulties which mode-coupling theories meet at short length scales [34,35]. Remarkably, the scaling works nicely for τ_1 over more than three orders of magnitude with an exponent $\gamma = 1.47 \pm 0.01$. This parallels the scaling which was noted for the translation diffusion coefficient and the primary relaxation time τ_α in I. For $0.7 < T < 2$ the quantities $l(l+1)D_r\tau_l$ and $l(l+1)\tau_l/2\tau_1$ do not change appreciably and are in the range 1 – 2 in good agreement with the diffusion model which predicts that both of them equal to 1 independently of the temperature. For $T < 0.7$ the above quantities increase abruptly. The increase of the quantity $l(l+1)\tau_l/2\tau_1$ is reasonably accounted for by the jump-rotation model for $l = 2$ [32]. For higher l values the agreement becomes quite poor. Being τ_1 and τ_2 measured by most experiments [2-5,28,42] this finding may account for the attention that the jump model has attracted during the last years [31,43,44].

The analysis of the angular Van Hove function evidences that in this region a meaningful fraction of the sample reorients by jumps of about 180° . The flips are rather fast and exhibit no meaningful distribution of both the amplitude and the time needed to complete a jump. Differently, it was noted in I that translational jumps require different times to be performed. The absence of a similar effect for the reorientations indicates a larger angular freedom. This is also apparent by the larger number of rotational jumps which are detected with respect to the translational ones. It is worth noting that the ease to jump does not lead to trivial relaxation properties, as signaled by the stretched decay of $C_{1,2,3,4}$.

We characterized the distribution ψ_{rot} of the waiting-times in the angular sites. It vanishes exponentially at long times whereas at lower temperatures it decays at short times as $t^{\xi-1}$ with $\xi = 0.34 \pm 0.04$ at $T = 0.5$. Interestingly, the translational waiting-time distribution exhibits the same behavior (see I). The exponent for the translational case is $\xi = 0.49$. We ascribe the power-law to the intermittent features of the motion in glassy systems [36-39].

The intermittent jump reorientation is fairly different from the motion in a liquid. Then, a decoupling from the viscous flow and the subsequent breakdown of the Debye-Stokes-Einstein is anticipated. Our study confirms the breakdown and shows that the quantity η/XkT with $X = D_r^{-1}, l(l+1)\tau_l$ and $l = 1-4$ diverges below $T = 1$. In particular, the correlators being affected by rotational jumps, e.g. $C_{1,3}(t)$, yield correlation times fairly more decoupled by the viscosity. A rather similar decoupling was found in I for the product $D\eta$, D being the translational diffusion coefficient.

The decoupling of the molecular reorientation by the viscosity could be also anticipated by the observed ease to perform rotational jumps. The reduced tendency to freeze of the rotational degrees of freedom was pointed out by MD [9] and theoretical [6] studies. The former in-

vestigating the residual rotational relaxation in a random lattice with *quenched translations* and the latter predicting a hierarchy for the glassy freezing, i.e. the rotational dynamics can never freeze *before* the translational dynamics. The decoupling of the rotational motion of guest molecules from the viscous flow has been experimentally seen by time-resolved fluorescence [27,28] and Electron Spin Resonance [5,29,30] while photobleaching and NMR studies reported small deviations from DSE even close to T_g [2,3]. It is worth noting that the decoupling of the translational diffusion from the viscosity and related phenomena as the so-called rotation-translation paradox have been ascribed to a spatial distribution of mobility and relaxation properties, so called dynamical heterogeneities [2,4,45–49]. Their role will be addressed in a forthcoming study.

ACKNOWLEDGMENTS

The authors warmly thank Walter Kob for having suggested the investigation of the present model system and the careful reading of the manuscript. Umberto Balucani, Claudio Donati and Francesco Sciortino are thanked for many helpful discussions and Jack Douglas for a preprint of ref. [39].

* corresponding author: e-mail address:
leporini@mailbox.difi.unipi.it.

- [1] for a short review see: M.D.Ediger, C.A.Angell, S.R.Nagel *J.Phys.Chem.***100**,13200 (1996).
- [2] M.T. Cicerone, F.R.Blackburn, M.D.Ediger *J.Chem.Phys.*, **102**, 471 (1995); M.T. Cicerone, M.D.Ediger *J.Chem.Phys.*, **104**, 7210 (1996).
- [3] F. Fujara, B.Geil, H.Sillescu, G.Fleischer *Z.Phys.* **B88**, 195 (1992); I.Chang, F.Fujara, B.Geil, G.Heuberger, T.Mangel, H.Sillescu *J.Non-Cryst.Solids* **172-174** 248 (1994).
- [4] D.B.Hall, A.Dhinojwala, J.M.Torkelson *Phys.Rev.Lett.* **79**, 103 (1997).
- [5] L.Andreozzi, A.Di Schino, M.Giordano, D.Leporini, *Europhys.Lett.* **38**, 669 (1997).
- [6] R.Schilling, T.Scheidsteger *Phys. Rev. E* **56**, 2932 (1997).
- [7] T.Franosch, M.Fuchs, W.Götze, M.R.Mayr, A.P.Singh *Phys. Rev. E* **56**, 5659 (1997); W.Götze *J.Phys.:Condens.Matter*, **11**, A1 (1999); H.Z.Cummins *J.Phys.:Condens.Matter*, **11**, A95 (1999).
- [8] G.Diezemann, H.Sillescu, G.Hinze, R.Böhmer *Phys. Rev. E* **57**, 4398 (1998);
- [9] S.Ravichandran, B.Bagchi *Phys.Rev.Lett.* **76**, 644 (1996).
- [10] S.Kämmerer, W.Kob, R.Schilling *Phys.Rev.E* **56** 5450 (1997).
- [11] S.Kämmerer, W.Kob, R.Schilling *Phys.Rev.E* **58** 2141 (1998).
- [12] S.Kämmerer, W.Kob, R.Schilling *Phys.Rev.E* **58** 2131 (1998).
- [13] Proceedings of the II Workshop on Non-Equilibrium Phenomena in Supercooled Fluids, Glasses and Amorphous Materials, M.Giordano, D.Leporini, M.P.Tosi (eds.). *J.Phys.:Condens.Matter*, Vol.11, No.10A (1999).
- [14] for a review see W.Kob, *J.Phys.:Condens.Matter* **11** R85 (1999).
- [15] G.F.Signorini, J.-L.Barrat *J.Chem.Phys* **92** , 1294 (1990).
- [16] L.J.Lewis, G.Wahnström, *J.Non-Cryst.Solids* **172-174**, 69 (1994); *Phys.Rev.E* **50** , 3865 (1994) .
- [17] S.R.Kudchakar, J.M.Wiest *J.Chem.Phys* **103**, 8566 (1995).
- [18] P.Sindzingre, M.L.Klein *J.Chem.Phys* **96** , 4681 (1992).
- [19] P.Gallo, F.Sciortino, P.Tartaglia, S.-H.Chen *Phys.Rev.Lett.* **76** , 2730 (1996); S.-H.Chen, P.Gallo, F.Sciortino, P.Tartaglia *Phys.Rev. E* **56** , 4231 (1997); F.Sciortino, L.Fabbian, S.-H.Chen, P.Tartaglia *Phys.Rev. E* **56** , 5397 (1997).
- [20] C.Renner, H.Löwen, J.L.Barrat *Phys.Rev.E* **52** , 5091 (1995).
- [21] S.J.Lee, B.Kim *Phys.Rev.E* **60** , 1503 (1999).
- [22] C.De Michele, D.Leporini submitted to *Phys. Rev. E*.
- [23] S.Glasstone, K.J.Laidler, H.Eyring, *The Theory of Rate Processes* (McGraw-Hill, New York, 1941).
- [24] H.Lamb *Hydrodynamics* VI Ed. (Cambridge University Press, Cambridge 1932).
- [25] L.D. Favro *Phys.Rev.* **119** , 53 (1960).
- [26] C.-M. Hu, R.Zwanzig *J.Chem.Phys.* **60** , 4354 (1974).
- [27] J.Y.Ye, T.Hattori, H.Nakatsuka, Y.Maruyama, M.Ishikawa, *Phys.Rev.B* **56**, 5286 (1997)
- [28] J.C.Hooker, J.M.Torkelson, *Macromolecules*, **28**, 7683 (1995).
- [29] L.Andreozzi, M.Giordano, D.Leporini, *J. of Non Cryst. Solids*, **235-237**, 219 (1998).
- [30] M.Faetti, M.Giordano, L.Pardi, D.Leporini *Macromolecules*, **32** 1876 (1999)
- [31] L.Andreozzi, F.Cianflone, C.Donati, D.Leporini *J.Phys.: Condens.Matter* **8**, 3795 (1996)
- [32] E.N.Ivanov *Soviet Physics JETP*, **18**, 1041 (1964); K.A.Valiev, E.N.Ivanov *Sov.Phys.-Usp*, **16**, 1 (1973).
- [33] J.-P.Hansen, I.R. McDonald *Theory of Simple Liquids* II Edition (Academic Press, London 1986).
- [34] T.Franosch, W.Götze *Phys.Rev.E* **57**, 5833 (1998).
- [35] U.Balucani, M.Zoppi, *Dynamics of the Liquid State*, (Clarendon, Oxford, 1994).
- [36] L.Sjögren *Z.Phys.B* **74**, 353 (1989).
- [37] J.F.Douglas, J.B.Hubbard *Macromolecules* **24**, 3163 (1991); J.F.Douglas *Comp.Mat.Sci.* **4**, 292 (1995).
- [38] T.Odagaki *Phys.Rev.Lett.* **75**, 3701 (1995).
- [39] P.Allegri, J.F.Douglas, S.H.Glotzer submitted to *Phys.Rev.E*.
- [40] T.Muranaka, Y.Hiwatari, *J.Phys.Soc of Japan*, **67** 1982 (1998).
- [41] R.Hilfer, L.Anton *Phys.Rev.E* **51**, R848 (1995).
- [42] N.G.McCrum, B.E.Read, G.Williams *Anelastic and Dielectric Effects in Polymeric Solids* (Wiley, New York,

- 1967).
- [43] G.Williams, P.J.Hains *J.Chem.Soc.Faraday Symp.* **6** , 14 (1972).
 - [44] M.S.Beevers, J.Crossley, D.C.Garrington, G.Williams *J.Chem.Soc.Faraday Trans. II* **73** , 458 (1977).
 - [45] J. A. Hodgdon, F. H. Stillinger *Phys.Rev.E* **48**, 207 (1993); F. H. Stillinger, J. A. Hodgdon *ibid.* **50**, 2064 (1994);
 - [46] C.Z.-W. Liu, I.Oppenheim,*Phys.Rev.* **E53**, 799 (1996).
 - [47] J.F.Douglas, D.Leporini *J.Non-Cryst.Solids* **235-237**, 137 (1998).
 - [48] H.Sillescu *J.Non-Cryst.Solids* **243**, 81 (1999).
 - [49] W.Kob, C.Donati, S.J.Plimpton, P.H.Poole, S.C.Glotzer *Phys.Rev.Lett.* **79** 2827 (1997); C.Donati, j.F.Douglas, W.Kob, S.J.Plimpton, P.H.Poole, S.C.Glotzer *Phys.Rev.Lett.* **80** 2338 (1998).